



Human bocavirus 1 and 2 genotype-specific antibodies for rapid antigen testing in pediatric patients with acute respiratory infections

Ri De¹ · Yan-Peng Xu^{1,2} · Fang Wang¹ · Yu-Tong Zhou¹ · Pan-Deng Shi² · Ru-Nan Zhu¹ · Yu Sun¹ · Li-Ying Liu¹ · Li-Ping Jia¹ · Hui-Jin Dong¹ · Hui Zhao² · Cheng-Feng Qin² · Lin-Qing Zhao¹

Received: 11 July 2022 / Accepted: 29 January 2023 / Published online: 22 February 2023
© Children's Hospital, Zhejiang University School of Medicine 2023

Abstract

Background Previous serological studies of human bocavirus (HBoV) 1 could not exclude cross-reactivity with the other three HBoVs, particularly HBoV2.

Methods To search for genotype-specific antibodies against HBoV1 and HBoV2, the divergent regions (DRs) located on the major capsid protein VP3 were defined through viral amino acid alignment and structure prediction. DR-deduced peptides were used as antigens to harvest corresponding anti-DR rabbit sera. To determine their genotype specificities for HBoV1 and HBoV2, these sera samples were used as antibodies against the antigens VP3 of HBoV1 and HBoV2 (expressed in *Escherichia coli*) in western blotting (WB), enzyme-linked immunosorbent assay (ELISA), and bio-layer interferometry (BLI) assays. Subsequently, the antibodies were evaluated with clinical specimens from pediatric patients with acute respiratory tract infection by indirect immunofluorescence assay (IFA).

Results There were four DRs (DR1–4) located on VP3 with different secondary and tertiary structures between HBoV1 and HBoV2. Regarding the reactivity with VP3 of HBoV1 or HBoV2 in WB and ELISA, high intra-genotype cross-reactivity of anti-HBoV1 or HBoV2 DR1, DR3, and DR4, but not anti-DR2, was observed. Genotype-specific binding capacity of anti-DR2 sera was confirmed by BLI and IFA, in which only anti-HBoV1 DR2 antibody reacted with HBoV1-positive respiratory specimens.

Conclusion Antibodies against DR2, located on VP3 of HBoV1 or HBoV2, were genotype specific for HBoV1 and HBoV2, respectively.

Keywords Divergent regions · Genotype-specific antibody · Human bocavirus 1 and 2 · Major capsid protein VP3

Introduction

Human bocavirus (HBoV) 1 was first identified in nasopharyngeal aspirates (NPAs) from children with respiratory tract infection in 2005 by Allander et al. through new nucleic acid-based techniques, metagenomic detection systems, for

active virus hunting, which paved the way for virus discoveries [1]. In close succession, three HBoVs (HBoV2, 3, and 4) were similarly detected in 2008–2010 in human stool samples when scientists searched for new viruses responsible for gastroenteritis [2, 3]. In addition to stool samples and NPAs, these viruses have been detected in serum, cerebrospinal fluid, sewage, and river water [4, 5]. The causative role of HBoVs in respiratory and enteric pathology is under investigation, which is a long journey full of potential pitfalls [6, 7]. In fact, the tissue tropisms of HBoV1 and HBoV2 were different, as evidenced by their different detection frequencies in different clinical samples and patients, resulting in the identification of HBoV1 as the human respiratory bocavirus and HBoV2 as the human enteric bocavirus [4, 8, 9].

All HBoVs are members of the family *Parvoviridae*, subfamily *Parvovirinae*, and genus *Bocaparvovirus*, with linear single-stranded DNA genomes encoding non-structural

✉ Cheng-Feng Qin
qincf@bmi.ac.cn

✉ Lin-Qing Zhao
linqingz525@163.com

¹ Laboratory of Virology, Beijing Key Laboratory of Etiology of Viral Diseases in Children, Capital Institute of Pediatrics, Beijing 100020, China

² State Key Laboratory of Pathogen and Biosecurity, Beijing Institute of Microbiology and Epidemiology, Academy of Military Medical Sciences, Beijing 100071, China

proteins NS1–4 and NP1 and capsid structural viral proteins VP1–3 [10–12]. The three capsid proteins VP1–3 share a common C terminus, with an expression ratio of 1:1:10, to form a non-enveloped icosahedral capsid, which was structured as depressions at the twofold axis, protrusions surrounding the threefold axis, and a canyon surrounding a channel at the fivefold axis of symmetry.

The HBoV capsid carries host and tissue tropism determinants and domains for pathogenicity, genome packaging, assembly, and antigenicity required for viral infection [13]. In HBoV1, the major capsid protein VP3 can assemble virus-like particles (VLPs) containing neutralizing epitopes and receptor binding sites [14]. The variable surface region (VR) III (²⁰²LDGNAAGG²⁰⁹) of HBoV1 VP3 has been proposed as a relevant factor of tissue tropism. These regions in enteric HBoV2 VRIII (²⁰²MEDA²⁰⁵) and HBoV3–4 VRIII (²⁰²MEDS²⁰⁵) are structurally similar but different from those of respiratory HBoV1 [15, 16]. These observations suggest that this region might be an important determinant of the genotype specificity of HBoV1 and HBoV2.

Serological studies have used recombinant HBoV1 capsid proteins as antigens to establish causal relationships between acute respiratory tract infection (ARTI) and HBoV1 based on seroconversion or an increase in immunoglobulin G (IgG) level \geq fourfold, which could not exclude cross-reactivity with the capsid proteins of the other three HBoVs, particularly HBoV2, resulting in the original antigenic sin (OAS) phenomenon due to the absence of genotype-specific antibodies [17, 18]. Although monoclonal antibodies against HBoV1 and HBoV2 have been previously reported, they have not been tested in clinical specimens [13]. To search for genotype-specific antibodies, the divergent regions (DRs) on VP3 were aligned, and antibodies targeting DRs of HBoV1 or HBoV2 VP3 were harvested and evaluated by western blotting (WB), enzyme-linked immunosorbent assay (ELISA) and bio-layer interference (BLI), followed by indirect immunofluorescence assay (IFA) with clinical samples.

Methods

Searching for DRs between HBoV1 and HBoV2 by amino acid sequence alignment and structure prediction

Genomic sequences of HBoV1 and HBoV2 from countries around the world were downloaded from GenBank and numbered with their GenBank number, country and year [19, 20]. Phylogenetic analysis was conducted using the neighbor-joining method and maximum composite likelihood model by MEGA7.0 and Clustal X to align

VP3 amino acid sequences. Based on DR data of the VP3 gene, the residues exposed on the surface of VP3 from ABK32030.1 and AFW98869.1 reported by our laboratory in Beijing, belonging to HBoV1 or HBoV2, respectively, were predicted by ProtScale (<https://web.expasy.org/protscale/>). The helix, turn, random coil, and extend stand were analyzed using Jpred4 (<http://www.compbio.dundee.ac.uk/jpred/index.html>) to obtain this VP3 secondary structural information. The antigenic index of the proteins was predicted in the Jameson-Wolf method by DNASTar Protean software. The tertiary structure model of VP3 was predicted by Swiss-Model (<https://swissmodel.expasy.org>) homology modeling according to the homologous template, named HBoV1–7L0W and HBoV2–7L0U in the Protein Data Bank (<http://www.wwpdb.org>). By PyMOL (<https://pymol.org/2/>), the VP3 tertiary structure models were visualized and searched for regions with a significant difference at the amino acid level of VP3 between HBoV1 and HBoV2.

Synthesis of peptides according to the DRs of VP3 from HBoV1 and HBoV2 for specific antibody preparation

Peptides deduced from the DRs of VP3 from HBoV1 and 2 were synthesized by GL Biochem (Shanghai, China), with expecting purity > 98%, and kept at -80°C . These peptides were then dissolved in 8 M urea–phosphate-buffered saline (PBS) buffer for immunization of 6- to 8-week-old clean Japanese white rabbits from Hubei province of China ($n=2$ per group) with Freund's adjuvant using the following doses of 0.7, 0.35, 0.35, 0.35, and 0.25 μg on weeks 0, 2, 4, 6 and 8, respectively, for specific antibody preparation, while PBS was used in the control group ($n=2$ per group). Blood samples were then collected from the marginal auricular vein of rabbits at weeks 0 (before primary immunization), 2, 4, 6, and 8. Finally, all rabbits were euthanized at week 8 for serum collection.

Expression and purification of VP3

Recombinant VP3 of HBoV1 and HBoV2 was expressed in *Escherichia coli* (*E. coli*) as previously described [21]. In brief, the coding regions of the HBoV1 VP3 gene (nt 3443–5071 of ABK32030.1) and HBoV2 VP3 gene (nt 3426–5042 of AFW98869.1) were amplified and cloned into the expression vector PET30b and transformed into *E. coli* DH5 α for the selection of positive clones. Then, the recombinant plasmids PET30b-HBoV1 VP3 or PET30b-HBoV2 VP3 were transformed into *E. coli* BL21 (DE3) (Novagen, USA) and induced by 1 mmol/L isopropyl- β -D-thiogalactopyranoside for 19 hours. VP3 was harvested mostly in inclusion bodies with an N-terminal 6 \times His tag

downstream of the T7 promoter, yielding a protein with a molecular weight of 68 kDa. After ultrasonication, the expressed VP3 was subjected to partial affinity purification with nickel-nitrilotriacetic acid agarose (Qiagen, USA).

Western blotting

Purified VP3 proteins were separated by 8%–20% SDS–PAGE and then transferred to nitrocellulose membranes. After blocking with 5% non-fat dry milk solution in TBST (Tris–HCl, 0.5% Tween-20) at room temperature for 2 hours, the membranes were incubated with antibodies against peptides of VP3 prepared in the study at 4 °C overnight. On the next day, the membranes were washed three times in TBST and then incubated with horseradish peroxidase (HRP)-conjugated goat anti-rabbit IgG antibodies (Zhongshan, China) at room temperature for 1 hour. The color was developed by addition of the Luminata Forte Western HRP Substrate, and the intensity of the immunoblot bands was quantified using a System GelDoc XR + ImageLab.10⁻⁸.

Enzyme-linked immunosorbent assay

The concentration of purified VP3 was determined by the Bradford Protein Quantitative Kit (Sangon Biotech No. C503031) according to the standard curve of bovine serum albumin with an absorption wavelength of A595. Subsequently, 50 µL per well of purified VP3 (2 µg/mL, diluted in PBS) was coated onto 96-well microplates for incubation overnight at 4 °C. After blocking with 5% non-fat dry milk solution in TBST at 37 °C for 1 hour, 50 µL per well of antibodies against peptides (5 µg/mL, by double dilution) were added to each well and incubated at 37 °C for 1 hour, followed by incubation at 37 °C for 1 hour with 50 µL per well of HRP-conjugated goat anti-rabbit immunoglobulin G, (1:5000 dilution in TBST). Then, 3,3',5,5'-tetramethylbenzidine substrates were dispensed into wells and incubated at room temperature for 15 minutes, which was stopped by adding 100 µL per well of H₂SO₄. The absorbance was read using a spectrophotometer with a 450 nm filter. The cut-off value was determined as 2.1 times the value of the blank control.

Bio-layer interferometry assay

As a tool to assess the binding potency, a BLI assay [22] was chosen to detect the interaction of antibodies with HBoV1 VP3 (1.43 × 10³ nM) and HBoV2 VP3 (3.71 × 10² nM). In brief, antibodies against HBoV1 DRs and HBoV2 DRs that showed no intra-genotype cross-reaction in WB and ELISA were double diluted. The purified VP3, anti-His-probe, and antibodies were added to the test tube according to the protocol. The kinetics module was run with the probes. The size of antibody affinity can be expressed

by the affinity constant K_d {L/mass molar concentration, $K_d = K_{off} \div K_{on} = [Ab \times H] / \{[Ab][H]\}$, and $R^2 \geq 0.95$ means effective detection.

Immunofluorescence assay

Anti-DR antibodies with no intra-genotype cross-reactivity in WB and ELISA were used in IFA. The specificity of anti-DR antibodies was tested using control slides of respiratory syncytial virus (RSV), influenza virus A and B (FluA and B), adenovirus (ADV), parainfluenza virus I, II, and III (PIV 1–3) from the D³ Ultra™ DFA Respiratory Virus Screening & ID Kit (Diagnostic Hybrids Inc., Athens, OH, USA) as antigens.

Clinical specimens (NPAs) were collected from pediatric patients hospitalized at the Capital Institute of Pediatrics, which were HBoV positive identified by viral screening using a capillary electrophoresis-based multiplex PCR (CEMP) assay (Ningbo HEALTH Gene Technologies Ltd., Ningbo, China) [23] and genotyped as HBoV1 by PCR [4]. These specimens were centrifuged at 500g for 10 minutes to have the cell pellets resuspended and spotted onto slides. These slides were then acetone fixed and kept at –20 °C for IFA.

For IFA, anti-DR antibodies diluted to 1:20, 1:40, and 1:80 were added to control or clinical specimen slides and then incubated at 37 °C for 30 minutes in a humidified box. The slides were washed three times in phosphate buffered saline with Tween-20 (PBST) and then incubated with fluorescein isothiocyanate (FITC)-conjugated goat anti-rabbit IgG antibodies (1:1000 dilution; Zhongshan, China) at 37 °C for 30 minutes. After three washes in PBST, the slides were observed under a fluorescence microscope (Nikon Eclipse 80i, Nikon Corporation, Japan).

Statistical analysis

All ELISA measurements were performed in triplicate for calculation of the mean values ± standard deviations using GraphPad Prism 9.0. Statistical analysis was conducted by one-way analysis of variance (ANOVA). *P* values < 0.05 were considered statistically significant.

Results

DRs on the amino acid sequences and structures of VP3 from HBoV1 and HBoV2

Based on the alignment of 31 reference amino acid sequences of HBoV1 VP3 (542 aa) and HBoV2 VP3 (538 aa), four regions with differences > 8 amino acids between HBoV1 and HBoV2 were named DR 1–4 (Supplementary Fig. 1a). The amino acids of DR2 were exposed more often

at the surface than those of DR1, 3, and 4 (Supplementary Fig. 1b). Comparison of the tertiary structural alignment and VP3 main chain region showed that DR1 of HBoV2 DR1, with a divergence of 12 amino acid mutations from HBoV1 DR1, formed a β -sheet independently, while HBoV1 DR4, with seven amino acid mutations, formed an extra α -helix. More importantly, HBoV2 DR2 (located on a fivefold region) formed an α -helix in addition to a β -turn and random coil with the deletion of four conserved amino acids (²⁰⁴GNAA²⁰⁷, located on a random coil between two α -helices of HBoV1 DR2), resulting in an incomplete loop that was exposed on the surface (Supplementary Fig. 1c). Using a value > 1 as a marker of high antigenic ability, DR1-DR4 all showed high antigenic indices and could be used as antigens for the development of specific antibodies (Table 1).

Intra-genotype cross-reactivity of antibodies specific to peptides deduced from DR1–4 of HBoV1 and HBoV2 in WB and ELISA

In WB, all immunoblot bands with a molecular weight of approximately 68 kDa were present when antibodies against DR1, 3, and 4 of HBoV1 and HBoV2 reacted with VP3 of HBoV1 or HBoV2, respectively. However, the bands were not detected when the anti-HBoV1 DR2 antibody was incubated with VP3 of HBoV2, and the

anti-HBoV2 DR2 antibody was incubated with VP3 of HBoV1 (Fig. 1a).

In ELISA, the half effective concentrations (EC_{50}) of anti-HBoV1 or anti-HBoV2 DR2 antibodies against HBoV1 VP3 ($7.271e-05$ and $2.192e-03$) and HBoV2 VP3 ($8.168e-04$ and $9.209e-05$) were different. The average OD450 values of the anti-HBoV1 DR1 antibody to HBoV1 and HBoV2 VP3 were 0.486 and 0.336 ($t = 1.743$, $P = 0.089$), respectively, and those of the anti-HBoV2 DR1 antibody to HBoV1 and HBoV2 VP3 were 0.646 and 0.600, ($t = 0.454$, $P = 0.653$), respectively, with no significant difference in these cross-reactivity assays. Similar results were observed in cross-reactivity assays of anti-DR3 and anti-DR4 antibodies. However, the average OD450 values of the anti-HBoV1 DR2 antibody were significantly higher in the reaction with HBoV1 VP3 (0.721) than in the reaction with HBoV2 VP3 (0.099) ($t = 7.382$, $P = 0.000$). The average OD450 values of the anti-HBoV2 DR2 antibody were significantly higher in the reaction with HBoV2 VP3 (0.701) than in the reaction with HBoV1 VP3 (0.121) ($t = 6.401$, $P = 0.000$) (Fig. 1b).

The binding ability of anti-HBoV1 or HBoV2 DR2 antibodies to VP3 in BLI assay

According to the BLI assay, as shown in Fig. 1c, the K_d , K_{on} , and K_{off} values of the anti-HBoV1 DR2 antibody to HBoV1VP3 were 8.78×10^{-9} (M), 7.64×10^4 (1/Ms), and

Table 1 Conformational information antigenic index of divergent region DR1–4 located on the major capsid protein VP3 of HBoV1 or HBoV2

Genotype	Divergent region	Mapped start–end	Sequence	Antigenic index	Length (mer)	Secondary structure	Surface accessibility
HBoV1	DR1	68–90	IQNGHLYKTEAIETTNQS-GKSQ	1.118	22	B sheet and β turn	Exposed
	DR2	195–220	IENELADLDGNAAGG-NATEKALLYQM	1.101/1.094	26	β turn, random coil and α helix	Exposed
	DR3	312–338	QSSDTAPFMVCTNPEGTH-INTGAAGFG	1.107	27	β turn and random coil	Exposed and buried
	DR4	523–542	IQPTSYPDQMPVKTNINKVL	1.104	20	β turn, random coil, α helix	Exposed
HBoV2	DR1	68–90	IQNDHKYRTENIIPSNAG-GKSQ	1.119	22	B sheet	Exposed
	DR2	195–216	VIHELAEEMEDAN-AVEKAIALQI	1.113	22	β turn, random coil and α helix	Exposed
	DR3	308–334	AGSDTASWMVVVNPDPG-TAVNSGMAGVG	1.135	27	β turn, random coil	Exposed and buried
	DR4	519–538	IQPTTWDMCYPIKTNINKVL	1.065	20	β turn, random coil	Exposed

Amino acid sequences of DR1–4 with high antigenic index were as follows. DR1: “IQN” of HBoV1 and HBoV2; DR2: “IEN” and “KALLYQM” of HBoV1, “VEKAIALQI” of HBoV2; DR3: “PFMVCTN” of HBoV1, “WMVVVNP” of HBoV2; DR4: “IQPTSYPDQMPVK” of HBoV1, “MCYPIK” of HBoV2. DR divergent region, VP capsid structural viral protein, HBoV human bocavirus

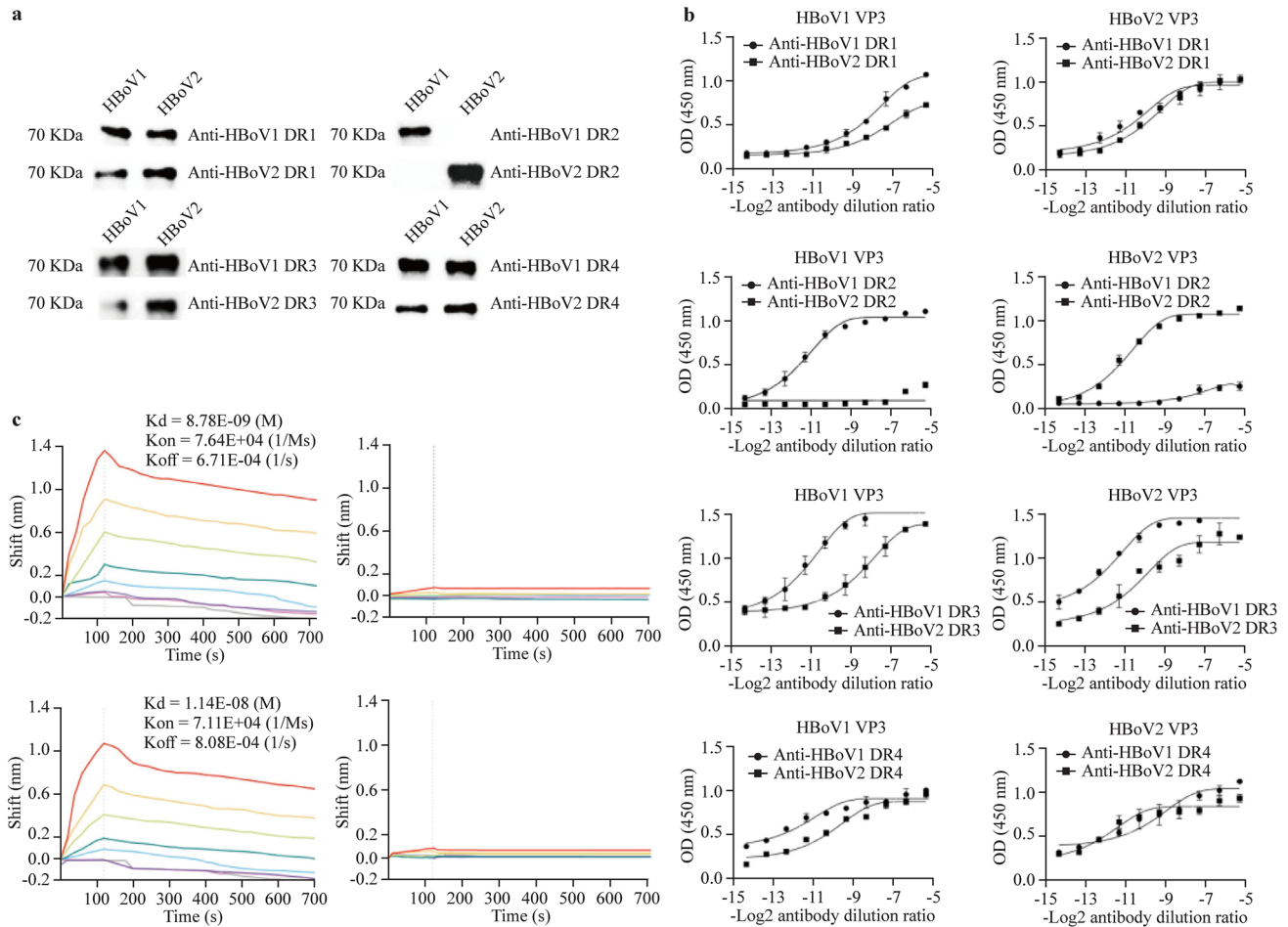


Fig. 1 Evaluating the genotypic specificity of anti-DRs in reacting with VP3 of HBoV1 or HBoV2 expressed in *Escherichia coli* BL21. **a** In western blotting, VP3 proteins of HBoV1 (lane HBoV1) or HBoV2 (lane HBoV2) expressed in *E. coli* BL21 was used as an antigen to react with antibodies labeled with anti-HBoV1 or HBoV2 DR1, DR2, DR3, and DR4. The immunoblot bands with a weight of about 68 kDa were shown when anti-DR1, 3, and 4 of HBoV1 and HBoV2 reacted with VP3 of HBoV1 or HBoV2, respectively, which were missed when anti-HBoV1 DR2 reacted with VP3 of HBoV2, as well as anti-HBoV2 DR2 reacted with VP3 of HBoV1; **b** in ELISA, VP3 (100 ng) of HBoV1 or HBoV2 expressed in *E. coli* BL21 were used as antigens to react with antibodies labeled with anti-HBoV1 or HBoV2 DR1, DR2, DR3, and DR4, respectively. The average OD450 values of anti-DR1, 3, and 4 to HBoV1 or HBoV2 VP3

showed no significant difference, while that of anti-DR2 to HBoV1 or HBoV2 VP3 showed a significant difference in these cross-reaction assays; **c** the binding curve graph of HBoV1 VP3 with anti-HBoV1 and anti-HBoV2 DR2, as well as HBoV2 VP3 with anti-HBoV1 and anti-HBoV2 DR2, calculated by Gator software. The highest concentration of polyclonal antibody was 250 nM in the red line. The other five colored lines indicate the ability of the twofold diluted antibody to bind to the VP3 antigen. The gray line indicates the blank control. The affinity constant K_d (unit is liter/mass molar concentration) was used to evaluate the size of antibody affinity $\{K_d = K_{off}/K_{on} = [Ab \times H]/([Ab][H])\}$. K_{off} dissociation rate constant, K_{on} the speed of intermolecular association, Ab antibody, H antigen, DR divergent region, VP capsid structural viral protein, $HBoV$ human bocavirus, $ELISA$ enzyme-linked immunosorbent assay

6.71×10^{-4} (1/s), while the K_d , K_{on} , and K_{off} values of the anti-HBoV2 DR2 antibody to HBoV1 VP3 could not be calculated by Gator, which showed no cross-reactivity. Similarly, the K_d , K_{on} , and K_{off} values of the anti-HBoV2 DR2 antibody to HBoV2 VP3 were 1.14×10^{-8} (M), 7.11×10^4 (1/Ms), and 8.08×10^{-4} (1/s), respectively. Additionally, the K_d , K_{on} , and K_{off} values of the anti-HBoV1 DR2 antibody to HBoV2 VP3 could not be calculated.

showed no significant difference, while that of anti-DR2 to HBoV1 or HBoV2 VP3 showed a significant difference in these cross-reaction assays; **c** the binding curve graph of HBoV1 VP3 with anti-HBoV1 and anti-HBoV2 DR2, as well as HBoV2 VP3 with anti-HBoV1 and anti-HBoV2 DR2, calculated by Gator software. The highest concentration of polyclonal antibody was 250 nM in the red line. The other five colored lines indicate the ability of the twofold diluted antibody to bind to the VP3 antigen. The gray line indicates the blank control. The affinity constant K_d (unit is liter/mass molar concentration) was used to evaluate the size of antibody affinity $\{K_d = K_{off}/K_{on} = [Ab \times H]/([Ab][H])\}$. K_{off} dissociation rate constant, K_{on} the speed of intermolecular association, Ab antibody, H antigen, DR divergent region, VP capsid structural viral protein, $HBoV$ human bocavirus, $ELISA$ enzyme-linked immunosorbent assay

Specific reaction of anti-HBoV1 DR2, not anti-HBoV2 DR2, antibodies to HBoV1-positive clinical specimens in IFA

Anti-HBoV1 and anti-HBoV2 DR2 antibodies showed negative results in reaction with control slides of RSV, Flu A and B, ADV, and PIV 1–3 in IFA. Three clinical specimens were tested in IFA. One specimen (D9466), collected on August

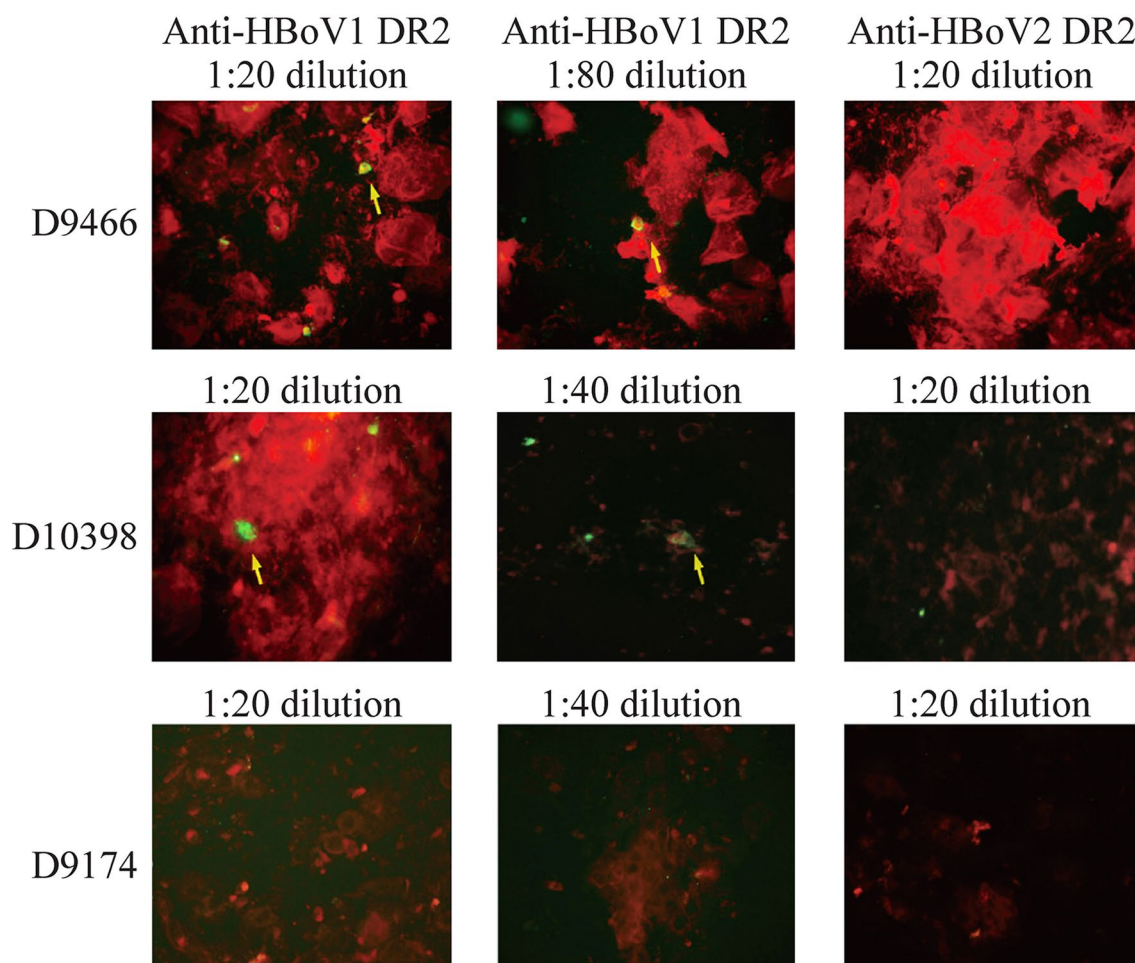


Fig. 2 The genotypic specificity of anti-HBoV1 DR2 was confirmed in the indirect immunofluorescence assay. Positive cells with specific green fluorescence (shown by arrows) were observed in clinical specimens (D9466 and D10398) reacting with anti-HBoV1 DR2

but not with anti-HBoV2 DR2. Only negative cells with no specific green fluorescence were shown in a clinical specimen (D9174) reacting with anti-HBoV1 and HBoV2 DR2. *DR* divergent region, *HBoV* human bocavirus

17, 2021, from a 14-month-old boy who was diagnosed with ARTI with the underlying disease of acute lymphoblastic leukemia, was positive for HBoV (6.11×10^4 copies/mL), RSV, and PIV determined by CEMP and then genotyped to HBoV1 by PCR, with PIV3 positivity and RSV negativity in IFA using individual FITC-labeled monoclonal antibodies against PIV3 or RSV, respectively, in the D³ Ultra™ DFA Respiratory Virus Screening & ID Kit. Another specimen (D10398), collected on November 23, 2021, from a 2-year-old girl who was diagnosed with pneumonia, was only positive for HBoV (6.13×10^4 copies/mL) determined by CEMP and then genotyped to HBoV1 by PCR. The third specimen (D9174), collected on July 19, 2021, from a 1-year 9-month-old girl who was diagnosed with pneumonia, was positive only for HBoV (5.85×10^4 copies/mL) determined by CEMP and then genotyped to HBoV1 by PCR.

In the reaction with NPAs D9466, more positive cells with specific green fluorescence were observed at a 1:20

dilution of anti-HBoV1 DR2 antibody than at a 1:80 dilution. Similarly, in the reaction with NPAs D10398, more positive cells were observed at the 1:20 dilution of anti-HBoV1 DR2 antibody than at a 1:40 dilution. However, no positive cells were observed in these clinical specimens in the reaction with the anti-HBoV2 DR2 antibody (Fig. 2). For D9174, no positive cells were detected in the reaction with either anti-HBoV1 or anti-HBoV2 DR2 antibodies.

Discussion

HBoVs possess three main structural proteins, VP1, VP2, and VP3, with an expression ratio of 1:1:10 of the virus capsid. Among these proteins, VP3, containing neutralizing epitopes and receptor binding sites, could be expressed as VLPs, which had good immunogenicity and induced highly specific antibodies in rabbits and mice [24]. However, the

lack of genotype specificity of antigens and antibodies in serological studies has led to cross-reactivity and the OAS phenomenon [17, 18]. This study searched the major viral capsid protein VP3 for its DRs between HBoV1 and HBoV2. Then, genotype-specific antibodies were harvested from rabbits immunized with peptides deduced from these DRs.

By comparison of 31 reference sequences, four DRs (DR1–4) in HBoV1 and HBoV2 were located on VP3, not only at the amino acid level with > 8 mutations but also at the secondary and tertiary structure levels. Notably, four conserved amino acids (²⁰⁴GNAA²⁰⁷) located at the apex of a half-loop structure in the form of a random coil between two α -helices were detected in HBoV1-DR2 (¹⁹⁵IENELADLDGNAAGGNATEKALLYQM²²⁰) but not in HBoV2-DR2 (¹⁹⁵VIHELAEEMEDANAVEKAIALQI²¹⁶), which is similar to those of HBoV1-VRIII (¹⁹⁸ELADLDGNAAGGNATEKALL²¹⁷) and HBoV2-VRIII (¹⁹⁶IHELAEEMED(A/S)NAVEKAI²¹²) [15].

To enhance the antigenic index, three amino acids (¹⁹⁵IEN¹⁹⁷) were added to HBoV1-DR2. The loss of the half-loop in the tertiary structure of HBoV2, which results from the deletion mutations of four amino acids in VP3, was also reported in HBoV3 and HBoV4 compared to that of HBoV1 at the apex of the loop by cryo-electron microscopy [15, 16]. Therefore, genotype specificity between HBoV1 and HBoV2 might be determined by DR2.

To harvest genotype-specific antibodies, peptides were synthesized according to the amino acid sequences of DR1–4, which were used as antigens to immunize rabbits for collection of anti-HBoV1 or anti-HBoV2 DR1–4 antibodies. Then, the genotype specificities of anti-HBoV1 or anti-HBoV2 DR1–4 antibodies in reaction with VP3 were tested by WB and ELISA. WB results showed high intra-genotype cross-reactivity of anti-HBoV1 or anti-HBoV2 DR1, 3, and 4 antibodies. However, anti-HBoV1 DR2 and anti-HBoV2 DR2 antibodies clearly showed no intra-genotype cross-reaction to VP3 of HBoV2 and HBoV1, respectively, which supported the hypothesis that the DR2 region might contain some genotype-specific features.

This hypothesis was further confirmed by ELISA. While the EC₅₀ values of anti-HBoV1 and anti-HBoV2 DR1, 3, and 4 antibodies showed no significant difference in reaction with VP3 of HBoV1 and HBoV2, the EC₅₀ of anti-HBoV1 and anti-HBoV2 DR2 antibodies showed a significant difference in reaction with VP3 of HBoV1 and HBoV2. The BLI assay was used as an efficient tool to determine the binding ability between antigens and antibodies. BLI results corroborated the intra-genotype specificity of anti-HBoV1 and anti-HBoV2 DR2 antibodies, which was further validated with the presence of positive cells in the reaction of HBoV1-positive NPAs from ARTI pediatric patients with anti-HBoV1 DR2 antibody but not anti-HBoV2 DR2 antibody.

The specimen D9174, which was positive for HBoV1 DNA, showed a negative result in the antigen test by IFA. Since PCR is more sensitive than immunofluorescence detection and shows positive results even in the incubation period and recovery periods, different detection methods should be selected at different disease stages. More complete collection of clinical history and laboratory data will improve the accuracy of the interpretation of the results. Our results also suggested that more large-scale antigen tests among ARTI pediatric patients can be carried out using these genotype-specific antibodies to build the correlation between HBoV1 and the disease.

In the specific reaction of anti-HBoV1 DR2 antibody to HBoV1-positive clinical specimens in IFA, only three samples with medium HBoV1 viral load were tested, which was a limitation of our study. Testing more clinical specimens, particularly those with or without concurrent detection of other pathogens and those with low, medium, or high viral loads, will provide a wider spectrum of results, which will empower a better understanding of HBoV1 infection and potential applications of the antibodies obtained in this work.

In conclusion, the genotype specificities of anti-HBoV1 and anti-HBoV2 DR2 antibodies were examined in WB and ELISA, which was strengthened by the absence of affinity of anti-HBoV1 and anti-HBoV2 DR2 antibodies to VP3 of HBoV2 and HBoV1, respectively, in BLI assay. Furthermore, these results were validated in HBoV1-positive clinical specimens, in which positive cells were detected only in reaction with anti-HBoV1 DR2 antibody, not with anti-HBoV2 DR2 antibody. Therefore, anti-HBoV1 and anti-HBoV2 DR2 antibodies can be used for rapid antigen tests in children's clinical samples and genotype-specific antibody detection in serological research, particularly in ARTI patients.

Supplementary Information The online version contains supplementary material available at <https://doi.org/10.1007/s12519-023-00697-8>.

Acknowledgements We would like to thank the Affiliated Children's Hospital and Capital Institute of Pediatrics staff for collecting the clinical samples, and the children and their parents who supported our research work. We would like to thank Editage (<http://www.editage.cn>) for language editing.

Author contributions DR contributed to methodology, formal analysis, and writing of the original draft. XYP contributed to validation, reviewing and editing. WF and ZYT contributed to data curation and methodology. SPD contributed to software. ZRN contributed to investigation. SY, LLY, JLP, and DHJ contributed to resources. ZH contributed to visualization. QCF contributed to supervision, project administration, reviewing and editing. ZLQ contributed to conceptualization, supervision, reviewing and editing, and funding acquisition. All the authors approved the final version of the manuscript.

Funding This work was supported by the Beijing Natural Science Foundation (7192029), the National Natural Science Foundation of

China (82172277), and the Beijing Municipal Commission of Health (2060399 PXM2017_026268_00005_00254486).

Data availability Data will be made available on reasonable request.

Declarations

Ethical approval The research was approved by the Ethics Committee of the Capital Institute of Pediatrics (approval number: SHER-LLM2019013) as a retrospective study.

Conflict of interest No financial or non-financial benefits have been received or will be received from any party related directly or indirectly to the subject of this article. The authors have no conflict of interest to declare.

References

- Allander T, Tammi MT, Eriksson M, Bjerkner A, Tiveljung-Lindell A, Andersson B. Cloning of a human parvovirus by molecular screening of respiratory tract samples. *Proc Natl Acad Sci U S A*. 2005;102:12891–6.
- Kapoor A, Slikas E, Simmonds P, Chieochansin T, Naeem A, Shaikat S, et al. A newly identified bocavirus species in human stool. *J Infect Dis*. 2009;199:196–200.
- Kapoor A, Simmonds P, Slikas E, Li L, Bodhidatta L, Sethabutr O, et al. Human bocaviruses are highly diverse, dispersed, recombination prone, and prevalent in enteric infections. *J Infect Dis*. 2010;201:1633–43.
- Zhao M, Zhu R, Qian Y, Deng J, Wang F, Sun Y, et al. Prevalence and phylogenetic analysis of human bocaviruses 1–4 in pediatric patients with various infectious diseases. *PLoS One*. 2016;11:e0160603.
- Kumthip K, Khamrin P, Ushijima H, Maneekarn N. The predominance of human bocavirus genotypes 1 and 2 in oysters in Thailand. *Appl Environ Microbiol*. 2021;87:e0045621.
- Qiu J, Söderlund-Venermo M, Young NS. Human parvoviruses. *Clin Microbiol Rev*. 2017;30:43–113.
- Söderlund-Venermo M. Emerging human parvoviruses: the rocky road to fame. *Annu Rev Virol*. 2019;6:71–91.
- Chieochansin T, Kapoor A, Delwart E, Poovorawan Y, Simmonds P. Absence of detectable replication of human bocavirus species 2 in respiratory tract. *Emerg Infect Dis*. 2009;15:1503–5.
- Arthur JL, Higgins GD, Davidson GP, Givney RC, Ratcliff RM. A novel bocavirus associated with acute gastroenteritis in Australian children. *PLoS Pathog*. 2009;5:e1000391.
- Shen W, Deng X, Zou W, Cheng F, Engelhardt JF, Yan Z, et al. Identification and functional analysis of novel nonstructural proteins of human bocavirus 1. *J Virol*. 2015;89:10097–109.
- Chen AY, Cheng F, Lou S, Luo Y, Liu Z, Delwart E, et al. Characterization of the gene expression profile of human bocavirus. *Virol*. 2010;403:145–54.
- Wang Z, Shen W, Cheng F, Deng X, Engelhardt JF, Yan Z, et al. Parvovirus expresses a small noncoding RNA that plays an essential role in virus replication. *J Virol*. 2017;91:e2375–416.
- Kailasa S, Garrison J, Ilyas M, Chipman P, McKenna R, Kantola K, et al. Mapping antigenic epitopes on the human bocavirus capsid. *J Virol*. 2016;90:4670–80.
- Zhao L, Qian Y, Ding Y, Zhu R, Deng J, Wang F, et al. The expression of the capsid protein VP2 from human bocavirus identified in Beijing and the formation of virus-like particles (VLPs) in insect cells. *Bing Du Xue Bao*. 2009;25:333–8 (in Chinese).
- Mietzsch M, Kailasan S, Garrison J, Ilyas M, Chipman P, Kantola K, et al. Structural insights into human bocaparvoviruses. *J Virol*. 2017;91:e00261–317.
- Luo M, Mietzsch M, Chipman P, Song K, Xu C, Spear J, et al. pH-induced conformational changes of human bocavirus capsids. *J Virol*. 2021;95:e02329–420.
- Kantola K, Hedman L, Allander T, Jartti T, Lehtinen P, Ruuskanen O, et al. Serodiagnosis of human bocavirus infection. *Clin Infect Dis*. 2008;46:540–6.
- Li X, Kantola K, Hedman L, Arku B, Hedman K, Söderlund-Venermo M. Original antigenic sin with human bocaviruses 1–4. *J Gen Virol*. 2015;96:3099–108.
- Zhao L, Qian Y, Zhu R, Deng J, Wang F, Li Y. Genomic sequence analysis for human Bocavirus circulating in Beijing by bioinformatics. *Zhonghua Weishengwuxue He Mianyixue Zazhi*. 2007;27:389–93 (in Chinese).
- Zhao H, Zhao L, Sun Y, Qian Y, Liu L, Jia LP, et al. Detection of a bocavirus circular genome in fecal specimens from children with acute diarrhea in Beijing, China. *PLoS One*. 2012;7:e48980.
- Zhao L, Qian Y, Dong H, Zhu R, Deng J, Li Y, et al. Prokaryotic expression and antigenicity of the capsid protein VP2 from human bocavirus identified in Beijing. *Zhonghua Weishengwuxue He Mianyixue Zazhi*. 2008;28:1–5 (in Chinese).
- Desai M, Di R, Fan H. Application of biolayer interferometry (BLI) for studying protein-protein interactions in transcription. *J Vis Exp*. 2019. <https://doi.org/10.3791/59687>.
- Li X, Chen B, Zhang S, Li X, Chang J, Tang Y, et al. Rapid detection of respiratory pathogens for community-acquired pneumonia by capillary electrophoresis-based multiplex PCR. *SLAS Technol*. 2019;24:105–16.
- Deng ZH, Hao YX, Yao LH, Xie ZP, Gao HC, Xie LY, et al. Immunogenicity of recombinant human bocavirus-1, 2 VP2 gene virus-like particles in mice. *Immunology*. 2014;142:58–66.

Publisher's Note Springer Nature remains neutral with regard to jurisdictional claims in published maps and institutional affiliations.

Springer Nature or its licensor (e.g. a society or other partner) holds exclusive rights to this article under a publishing agreement with the author(s) or other rightsholder(s); author self-archiving of the accepted manuscript version of this article is solely governed by the terms of such publishing agreement and applicable law.